Title

Cannabinoid Receptor Subtype-1 Regulates Allergic Airway Eosinophilia During Lung Helminth Infection

Permalink

https://escholarship.org/uc/item/1nc51427

Journal

Cannabis and Cannabinoid Research, 6(3)

ISSN

2578-5125

Authors

Wiley, Mark B
Bobardt, Sarah D
Nordgren, Tara M
et al.

Publication Date

2021-06-01

DOI

10.1089/can.2020.0167

Peer reviewed

Cannabinoid Receptor Subtype-1 Regulates Allergic Airway Eosinophilia During Lung Helminth Infection

Mark B. Wiley, Sarah D. Bobardt, Tara M. Nordgren, Meera G. Nair,[†] and Nicholas V. DiPatrizio[*,†]

Abstract

Introduction: Over 1 billion humans carry infectious helminth parasites that can lead to chronic comorbidities such as anemia and growth retardation in children. Helminths induce a T-helper type 2 (Th2) immune response in the host and can cause severe tissue damage and fibrosis if chronic. We recently reported that mice infected with the soil-transmitted helminth, *Nippostrongylus brasiliensis*, displayed elevated levels of endocannabinoids (eCBs) in the lung and intestine. eCBs are lipid-signaling molecules that control inflammation; however, their function in infection is not well defined.

Materials and Methods: A combination of pharmacological approaches and genetic mouse models was used to investigate roles for the eCB system in inflammatory responses and lung injury in mice during parasitic infection with *N. brasiliensis*.

Results: Hemorrhaging of lung tissue in mice infected with *N. brasiliensis* was exacerbated by inhibiting peripheral cannabinoid receptor subtype-1 (CB_1Rs) with the peripherally restricted CB_1R antagonist, AM6545. In addition, these mice exhibited an increase in nonfunctional alveolar space and prolonged airway eosinophilia compared to vehicle-treated infected mice. In contrast to mice treated with AM6545, infected cannabinoid receptor subtype-2-null mice ($Cnr2^{-/-}$) did not display any changes in these parameters compared to wild-type mice.

Conclusions: Roles for the eCB system in Th2 immune responses are not well understood; however, increases in its activity in response to infection suggest an immunomodulatory role. Moreover, these findings suggest a role for eCB signaling at CB_1Rs but not cannabinoid receptor subtypes-2 in the resolution of Th2 inflammatory responses, which become host destructive over time.

Keywords: cannabinoid; CB1R; eosinophil; helminth; infection; lung

Introduction

It is estimated that more than 1 billion humans are infected with helminths worldwide, with high prevalence in impoverished regions.[1] Infection with these parasites can lead to serious chronic comorbidities such as growth retardation and anemia.[1–3] In addition, infection leads to a T-helper type 2 (Th2) host immune response to enhance clearance; however, many parasitic infections are chronic in nature and require medical intervention.[4,5] Indeed, chronic tissue inflammation may lead to severe fibrosis and limit the functional capacity of the tissue. This Th2 response includes recruitment of several effector immune cells, including eosinophils, which contribute to the pathogenesis of allergies and asthma, and identifying factors that regulate this response is essential for improving therapeutics for parasitic infections.[6,7]

One model of parasitic infection used by our group and others is the soil-transmitted nematode, *Nippostrongylus brasiliensis*, which infects rodents through

Division of Biomedical Sciences, School of Medicine, University of California, Riverside, Riverside, California, USA.
[†]These two authors contributed equally.

*Address correspondence to: Nicholas V. DiPatrizio, PhD, Division of Biomedical Sciences, School of Medicine, University of California, Riverside, 900 University Avenue, Riverside, CA 92521, USA, E-mail: ndipatri@medsch.ucr.edu

similar mechanisms as soil-transmitted hookworms in humans.[2,8] Subcutaneous infection permits *N. brasiliensis* to enter circulation and migrate to the lungs by 2 days postinfection (DPI) where *N. brasiliensis* ingests host red blood cells to fuel their development, which can lead to anemia.[2]

Rodents infected with *N. brasiliensis* recruit several eosinophils to the site of infection to promote worm clearance, similar to what is seen in helminth infection in humans.[9] In addition, mice infected with *N. brasiliensis* display significant weight loss by 2 DPI coupled to a reduction in food intake, which is recovered by 5 DPI.[10] At 5–6 DPI, *N. brasiliensis* migrates up the trachea and down the esophagus into the small intestine (jejunum), where they establish adulthood in the intestinal phase of infection (7–8 DPI).[11] In the intestine, female *N. brasiliensis* releases fertilized eggs into the fecal matter for expulsion into the soil where the eggs hatch and their life cycle begins anew.[11]

We reported that *N. brasiliensis* infection was associated with increased levels of the endocannabinoids (eCBs) in infected organs (i.e., lung and jejunum epithelium), and pharmacological inhibition of eCB signaling at peripheral cannabinoid receptor subtype-1 (CB₁Rs) during the intestinal phase exacerbated metrics of infection, which suggests that CB₁R signaling may be host protective.[10] Consistent with these findings, longitudinal studies in humans showed associations between cannabis use and decreased helminth burden; however, whether the protective effect was from CB₁R signaling or a toxic effect of cannabis on the helminth is unclear.[12] In this study, we explored the role of endogenous cannabinoids (eCBs) in soil-transmitted helminth infections.

The eCBs, 2-arachidonoyl-*sn*-glycerol (2-AG) and anandamide, are bioactive lipids that bind and activate CB₁R and cannabinoid receptor subtype-2 (CB₂R) on cells throughout the body where they regulate numerous physiological functions, including inflammation.[13–15] Furthermore, these receptors are expressed on several immune cell subpopulations, including eosinophils.[16] Indeed, chemotaxis stimulated by interleukin-5 is enhanced in eosinophils that were cotreated with 2-AG in a CB₂R-dependent manner.[16,17] Pharmacological activation of CB₂Rs on eosinophils, however, failed to elicit the same response, suggesting a potential role for eicosanoids, which have been shown to contribute to eosinophil migration.[18] Moreover, genetic deletion of CB₁Rs and CB₂Rs had no effect on ovalbumin-stimulated lung eosinophilia in a mouse model of asthma, which suggests that eCB signaling at these receptors may not be required in associated allergic responses.[19] Nonetheless, activation of cannabinoid receptors on a variety of immune cells has been linked to immunosuppression; however, these effects are cell specific and context dependent.[20,21] Despite these limited studies, specific roles for the eCB system in parasitic infections remain largely unknown. We now investigated roles for the eCB system in inflammatory responses and lung injury during parasitic infection.

Materials and Methods

Mice and chemicals

C57BL/6 wild-type (WT) and Cnr2⁻/⁻ male mice were purchased from the Jackson Laboratory or bred in-house. All mice in experiments were age-matched (6- to 10-week-old) males given *ad libitum* access to a standard rodent chow. Mice were placed into single-housing units (TSE Systems, Chesterfield, MO) 3 days before recording feeding behavior to allow for acclimation. Daily feeding was monitored using PhenoMaster software (TSE Systems).

Mice in the CB₁R blockade experiments received intraperitoneal injections of vehicle control (7.5% dimethyl sulfoxide, 7.5% Tween 80, and 85% saline) or AM6545 (10 mg/kg/2 mL vehicle; Cayman Chemical, Ann Arbor, MI) 1 day before infection and everyday thereafter up to the day of harvest. All protocols for animal use and euthanasia were approved by the University of California Riverside Institutional Animal Care and Use Committee (protocols A-20200023 and A-20180023) and were in accordance with National Institutes of Health guidelines, the Animal Welfare Act, and Public Health Service Policy on Humane Care and Use of Laboratory Animals.

Infection

N. brasiliensis nematodes were obtained from the laboratory of Graham Le Gros (Malaghan Institute, New Zealand), and the life cycle was maintained in Sprague-Dawley rats (Harlan Laboratories) as previously described.[8,10] Rat fecal matter containing *N. brasiliensis* eggs was cultured for 1–2 weeks and hatched, and infectious L₃ larvae were recovered using Baermann apparatus. Mice were anesthetized with isoflurane and received a subcutaneous injection of 500–750 infective L₃ *N. brasiliensis* larvae suspended in 1×phosphate buffered saline (PBS). During the intestinal phase of infection (7–8 DPI) mice were euthanized using CO_2 asphyxiation, and the small intestine was removed

and cut longitudinally before incubating in $1 \times$ PBS at 37°C for 2 h to permit parasite migration out of the tissue. The number of worms was then manually quantified under a light microscope. Mice were placed into temporary single housing cages for 5–10 min (sufficient time for defecation to occur), and fecal matter was collected into preweighed tubes filled with $1 \times$ PBS. This mixture was homogenized, through pipetting, in a $1 \times$ PBS solution saturated with salt (NaCl), which permitted the eggs in the solution to float to the top. This mixture was added to the McMaster counting chamber for quantification under a light microscope as previously described.[4,8,10] The experimenter was blinded to conditions associated with counting worms and egg burden.

Tissue collection, sample processing, and flow cytometry

Cells recovered, at the time of harvest, from a bronchoalveolar lavage (BAL) were collected from both the left and right lungs through three sequential washes with 0.8 mL of $1 \times$ PBS. Two hundred microliters of the BAL fluid was quantified for hemorrhaging through plate reading using a Varioskan Lux (Thermo Scientific) at 540 nm as previously described.[22] The BAL fluid was treated with ammonium-chloride-potassium (ACK) lysis buffer, and cells were isolated by centrifugation. Blocking occurred using 10 μg/mL rat immunoglobulin G and 5 μg/mL anti-CD16/32 (2.4G2) and stained using antibodies (25 min, 4°C, 1:400 dilution in 50 μL fluorescence-activated cell sorting buffer) for SiglecF (E50-2440) and CD11c (N418) (all from BD Bioscience). Cells were washed then analyzed on an LSR II instrument (BD Biosciences), and data analysis was performed using FlowJo v10 (Tree Star, Inc.). Cell populations were identified as macrophages (CD11c$^+$ SiglecF$^+$) and eosinophils (CD11c$^-$SiglecF$^+$).

Histology

Lungs were recovered for histological sectioning as previously described.[4] Following recovery of the BAL fluid, lungs were inflated with fixative (0.8 mL): one part 4% paraformaldehyde (PFA)/30% sucrose in $1 \times$ PBS and two parts optimal cutting temperature embedding medium (Fisher Scientific). Recovery of the BAL fluid before inflation with fixative removed all blood cells from the lung air spaces; therefore, little to no red blood cells outside the vasculature were observed in the images. Lungs were stored for 24 h in 4% PFA (15 mL) followed by a 48 h incubation in 30% sucrose (20 mL). Lungs

were then blocked and sectioned at 8 μm and stained with hematoxylin and eosin. Sections were visualized under a DM5500B microscope (Leica).

Histological quantifications

One to three images per animal were taken at $4 \times$ in the lower left lobe of the left lung and used for all methods of image analysis. Infection with *N. brasiliensis* affects the whole lung and not specific regions[23]; therefore, the most easily identifiable region of the lungs (lower left lobe of the left lung) was chosen as the representative area to evaluate while ensuring consistency across all images. The investigator was blinded to conditions throughout all methods of analysis. Mean linear intercept (MLI) was performed as previously described.[24,25] Using QuPath open source software v0.2.1, a grid with x- and y-spacing maintained at 15 mm was laid across the image, and y-intercepts were manually counted across 10 lines. The MLI was calculated as follows:

$$\text{MLI} = \sum line \ lengths \ (mm) \div \sum intercepts$$

Nonfunctional alveolar space was quantitated using the same images used for MLI, and measurements (mm) of the nonfunctional space were performed using QuPath open source software's "wand tool" and "polygon" functions. Inclusion criteria: any open space not connected to an airway was included, and measurements $> 70.00 \ \text{mm}^2$ were included to ensure that nonpathological measurements were utilized. This method of analysis permitted for quantitation of average area of nonfunctional alveolar space and total area of nonfunctional alveolar space.

Statistical analysis

Data were analyzed by GraphPad Prism 8 software using unpaired Student's *t*-tests (two-tailed) and regular or repeated measures two-way analysis of variances with Newman–Keuls or Sidak's multiple comparisons *post hoc* test, respectively, when appropriate. Results are expressed as mean ± standard error of the mean, and significance was determined at $p < 0.05$.

Results and Discussion

CB$_1$R blockade exacerbates lung hemorrhaging in *N. brasiliensis* infection

Following subcutaneous infection, *N. brasiliensis* migrate into circulation and lodge themselves in the lung alveoli by 2 DPI, which bursts capillaries and causes extensive hemorrhaging and damage.[4,26] To
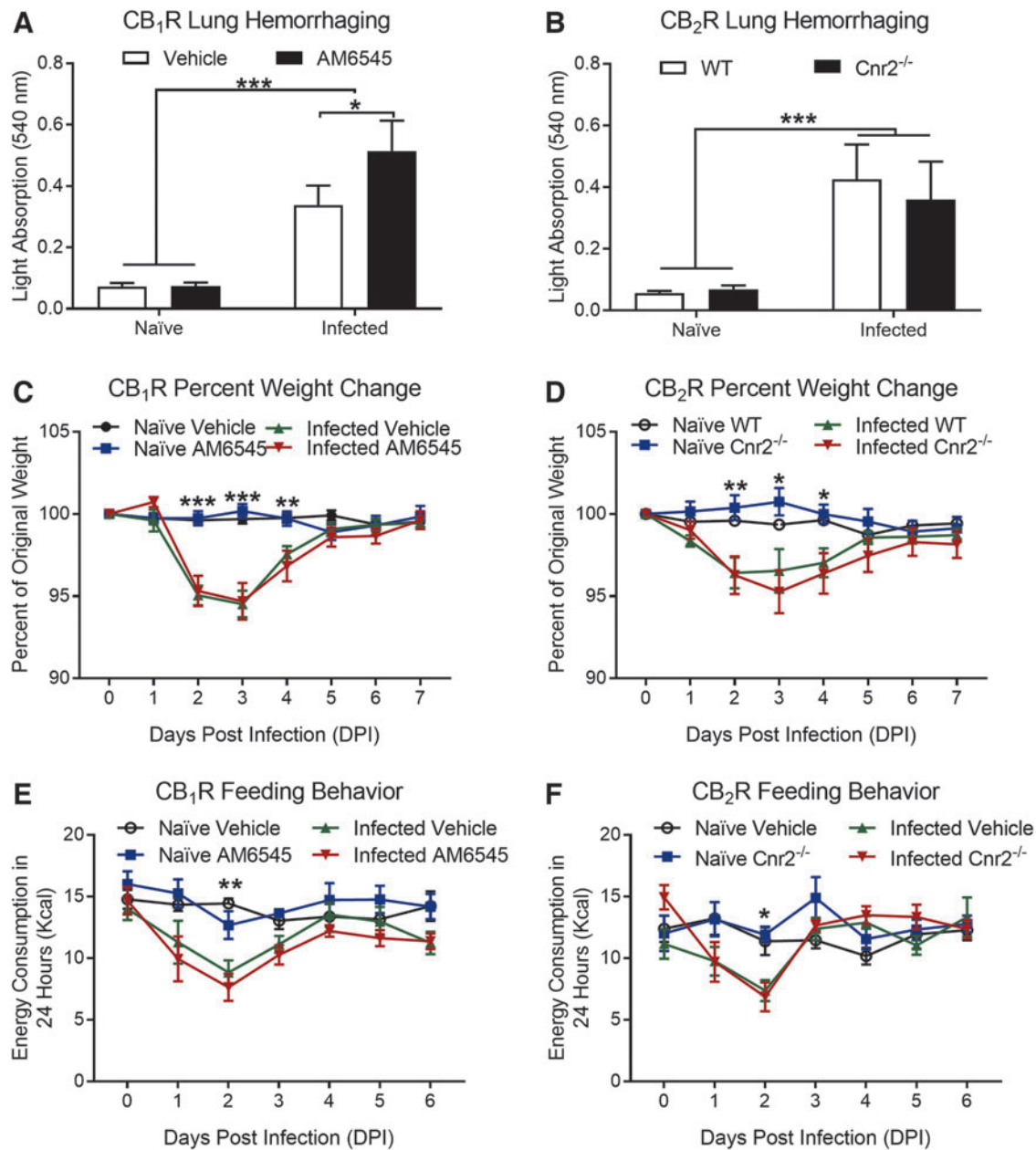
FIG. 1. Blockade of peripheral CB$_1$Rs with AM6545 exacerbated *Nippostrongylus brasiliensis* infection-induced lung hemorrhaging at 7 DPI compared to mice receiving vehicle treatment [**(A)**: $n = 19$, veh; $n = 21$, AM6545]. No changes in lung hemorrhaging occurred between infected CB$_2$R-null (Cnr2$^{-/-}$) and WT control mice [**(B)**: $n = 9$, WT; $n = 9$, Cnr2$^{-/-}$]. Mice infected with *N. brasiliensis* exhibited weight loss, which was unaffected by AM6545 or in CB$_2$R-null mice [**(D)**: $n = 9$, WT; $n = 9$, Cnr2$^{-/-}$] by 2 DPI. Body weights returned to baseline levels by 5 DPI. Similarly, energy consumption was reduced at 2 DPI, which returned to baseline by 4 DPI [**(E, F)**: $n = 14$, veh; $n = 14$, AM6545; $n = 9$, WT; $n = 9$, Cnr2$^{-/-}$]. Regular two-way ANOVA with Newman–Keul's multiple comparison *post hoc* test **(A, B)**; repeated measures two-way ANOVA with Sidak's multiple comparison *post hoc* test **(C–F)**; *p < 0.05, **p < 0.01, ***p < 0.001. Results are expressed as mean ± SEM. ANOVA, analysis of variance; CB$_1$R, cannabinoid receptor subtype-1; CB$_2$R, cannabinoid receptor subtype-2; DPI, days postinfection; SEM, standard error of the mean; WT, wild-type.

identify how CB_1Rs and CB_2Rs influence recovery from this lung damage, BAL samples collected in the intestinal phase of infection (7–8 DPI) were measured at 540 nm, which is a correlate for hemoglobin from hemorrhaging.[22] Compared to vehicle-treated mice infected with *N. brasiliensis*, blockade of peripheral CB_1Rs with the peripherally-restricted CB_1R antagonist, AM6545 (10 mg/kg), throughout *N. brasiliensis* infection exacerbated hemorrhaging (Fig. 1A, from 0.515 ± 0.099 AU to 0.338 ± 0.064 AU; $n = 21/19$, respectively, $p < 0.05$). Compared to infected WT mice, no changes in hemorrhaging were observed in infected $Cnr2^{-/-}$ mice (Fig. 1B, from 0.427 ± 0.111 AU to 0.359 ± 0.124 AU; $n = 9$, $p > 0.05$). Compared to naive mice, *N. brasiliensis* infection consistently caused weight loss as previously described (Fig. 1C, D).[10] However, no changes in infection-induced weight loss were observed in infected mice treated with AM6545, compared to vehicle treatment (Fig. 1C), or in global $Cnr2^{-/-}$ mice, compared to WT (Fig. 1D). The transient weight loss was coupled to hypophagia at 2 DPI and returned to baseline by 4 DPI regardless of treatment or genotype (Fig. 1E, F). Collectively, the results suggest that acute lung injury is exacerbated when peripheral CB_1Rs are inhibited throughout *N. brasiliensis* infection.
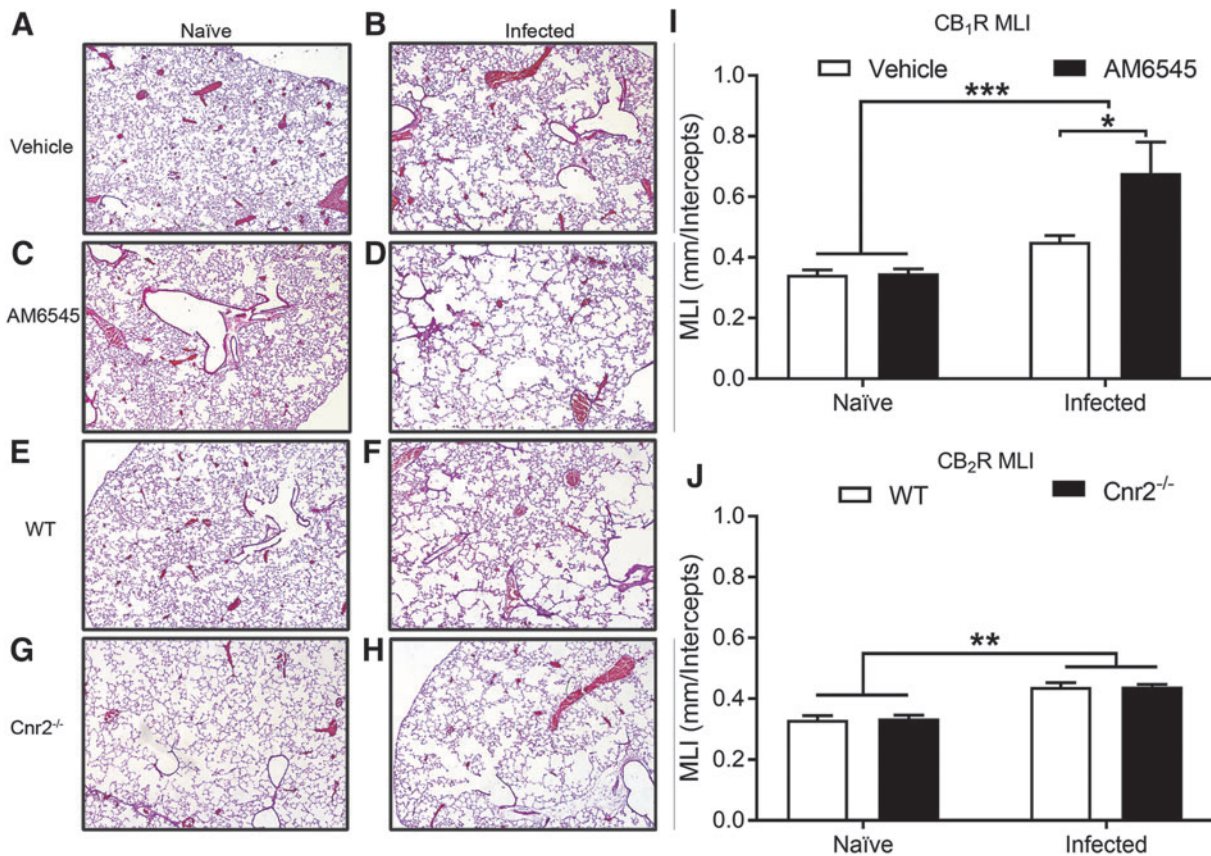

FIG. 2. Representative images of lung tissue damage in naive and infected mice receiving vehicle or AM6545 treatment **(A–D)** and in naive and infected WT and CB_2R-null mice **(E–H)**. Quantification of lung tissue damage was performed using MLI analysis, which indicates that peripheral blockade of CB_1Rs increased lung tissue damage in *N. brasiliensis* infection [**(I)**: $n = 13$, veh; $n = 14$, AM6545], while absence of CB_2Rs globally had no effect [**(J)** $n = 8$, WT; $n = 8$, $Cnr2^{-/-}$). Regular two-way ANOVA with Newman–Keul's multiple comparison *post hoc* test **(I, J)**; *$p < 0.05$, **$p < 0.01$, ***$p < 0.001$. Results are expressed as mean $\pm$ SEM. MLI, mean linear intercept.

CB₁R blockade exacerbates lung tissue damage

Infection with tissue-migrating *N. brasiliensis* results in extensive lung damage and disruption in the alveolar architecture as the parasite migrates through lung tissue. *N. brasiliensis* infection also has long-term pathologic consequences, including emphysema and fibrosis.[23] To identify if increased hemorrhaging in AM6545-treated mice was coupled to more severe lung tissue damage, multiple methods of image analysis were performed to evaluate lung alveolar architecture. Qualitatively, images of lung tissue samples used for image analysis in all groups (Fig. 2A–H) indicated less functional alveolar tissue throughout the lungs of *N. brasiliensis* infected mice, which appear to be further reduced in mice treated with AM6545. Representative images at a higher magnification (20×) are provided in the Supplementary Data (Supplementary Fig. S1A–

H). To provide quantitative evidence of reduced alveolar tissue, MLI analysis was performed on all groups tested, as previously described.[24,25] Compared to vehicle treatment, MLI was increased in *N. brasiliensis*-infected mice treated with AM6545 (Fig. 2I, from 0.451 ± 0.021 mm/int to 0.678 ± 0.103 mm/int; $n = 14/13$, respectively, $p = 0.0123$). In contrast to AM6545-treated mice, no change in MLI was found between infected WT and Cnr2$^{-/-}$ mice (Fig. 2J, from 0.439 ± 0.014 mm/int to 0.440 ± 0.007 mm/int; $n = 8$, $p = 0.937$). These data align with the extensive hemorrhaging observed in the AM6545-treated mice (Fig. 1A, B). To further validate changes in lung alveolar architecture, a second method of image analysis was performed. This method of quantitation confirmed that, compared to vehicle-treated mice infected with *N. brasiliensis*, infected mice treated with AM6545 displayed an
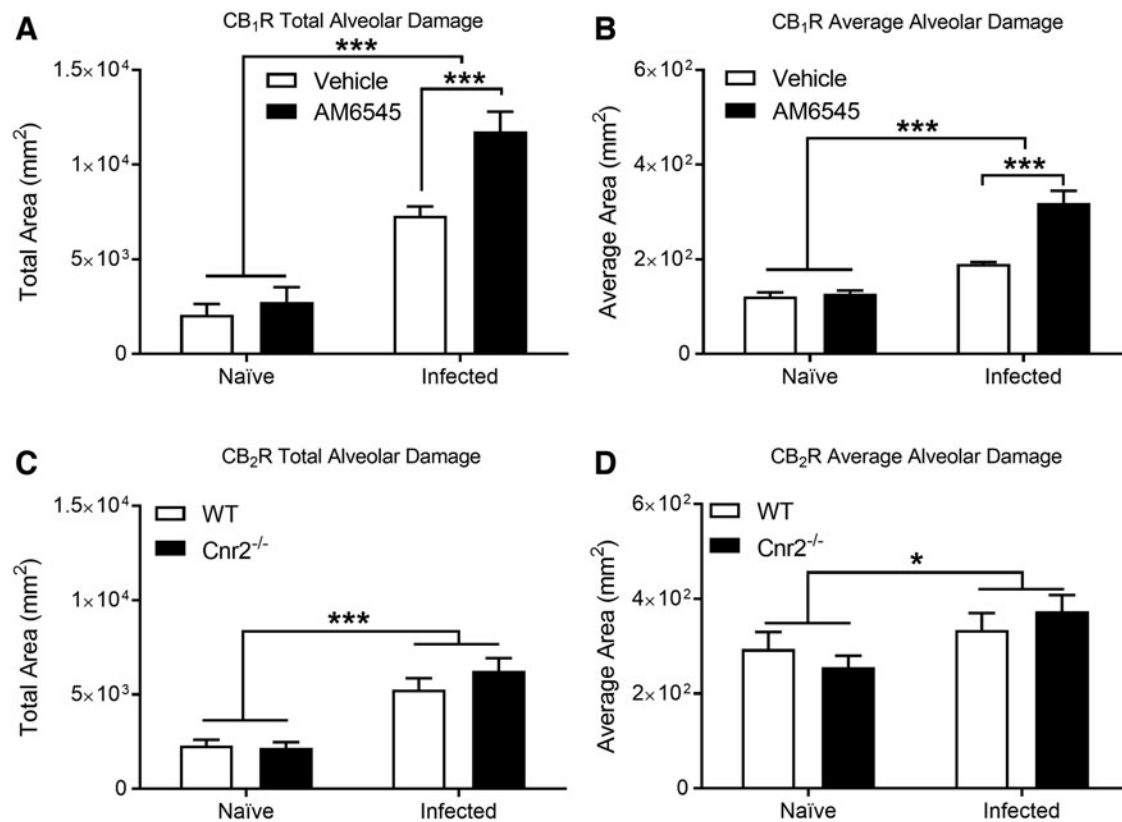

FIG. 3. Mice infected with *N. brasiliensis* that received AM6545 treatment displayed an increase in both average and total area of nonfunctional tissue compared to vehicle-treated mice infected with *N. brasiliensis* [**(A, B)**: $n = 13$, veh; $n = 14$, AM6545]. CB₂R-null mice displayed no change in these parameters compared to infected WT mice [**(C, D)**; $n = 8$]. Regular two-way ANOVA with Newman–Keul's multiple comparison *post hoc* test **(A–D)**; *$p < 0.05$, ***$p < 0.001$. Results are expressed as mean ± SEM.
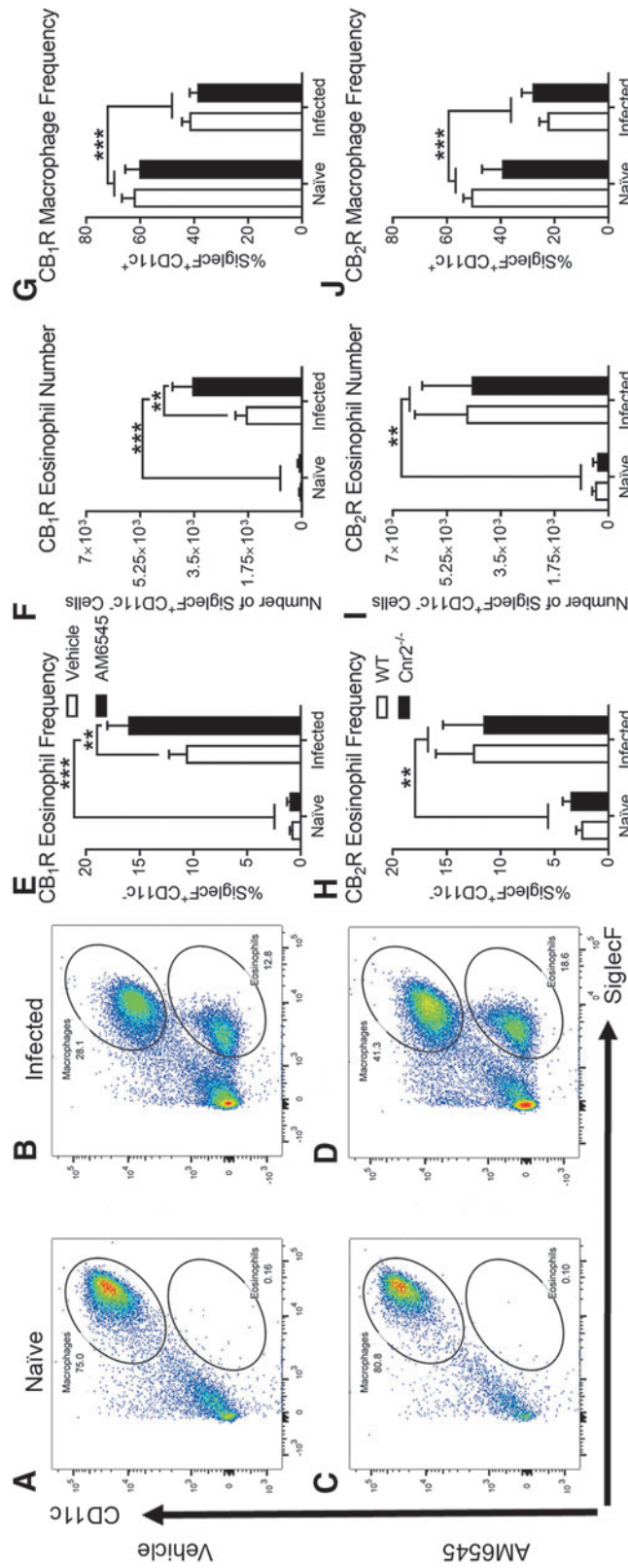
FIG. 4. Representative flow plots from cells collected in a bronchoalveolar lavage wash where airway macrophages (SiglecF⁺Cd11c⁺) were separated from eosinophils (SiglecF⁺Cd11c⁻) **(A–D)**. Mice infected with *N. brasiliensis* that received AM6545 treatment had increased raw number and percent of eosinophils (SiglecF⁺Cd11c⁻) compared to infected vehicle-treated mice infected with *N. brasiliensis* [**(E, F)**: $n = 20$, veh; $n = 21$, AM6545]. Infection with *N. brasiliensis* induced lung eosinophilia in both CB₂R-null and WT mice; however, no differences were observed across genotype [**(H, I)**: $n = 9$, WT; $n = 10$, Cnr2⁻/⁻]. Alveolar macrophages were the main cell population in naive mice, and frequency was reduced in *N. brasiliensis* infected samples [**(G, J)**: $n = 20$, veh; $n = 21$, AM6545; $n = 9$, WT; $n = 10$, Cnr2⁻/⁻]. Regular two-way ANOVA with Newman–Keul's multiple comparison *post hoc* test **(E–H)**; **p < 0.01, ***p < 0.001. Results are expressed as mean ± SEM.

increase in total and average nonfunctional alveolar space (Fig. 3A, total: from 7309 ± 482 mm^2 to $11,762 \pm 1,036$ mm^2, $p < 0.001$; Fig. 3B, average: from Avg: 190.2 ± 3.9 mm^2 to 318.7 ± 26.1 mm^2, $p < 0.001$). In contrast to AM6545-treated mice, no change in total and average nonfunctional alveolar space was found between infected WT and Cnr2$^{-/-}$ mice (Fig. 3C, total: from 5250 ± 623 mm^2 to 6254 ± 675 mm^2, $p = 0.329$; Fig. 3D, average: from 334.5 ± 35.9 mm^2 to 374.3 ± 33.8 mm^2, $p = 0.771$). Taken together, these data indicate that there was a decrease in functional alveolar tissue in mice treated with AM6545, caused either by increased infection-induced injury or a defect in alveolar tissue healing. Recent evidence suggests that overactivation of CB₁R in the lungs contributes to idiopathic pulmonary fibrosis, which appears to be alveolar macrophage mediated.[27] However, parasitic infections stimulate a Th2 immune response, which results in eosinophil recruitment and polarization of macrophages into alternatively activated macrophages, which are protective.[4,28,29] Thus, the role for CB₁R signaling in the lungs may depend on the inflammatory context, which inflammatory cell type is most prevalent, and the activation state of these cells.

Inhibition of peripheral CB₁Rs leads to increased airway eosinophilia

To identify if there was an inflammatory cell associated with the increase in lung tissue damage and hemorrhaging in response to *N. brasiliensis* infection, flow cytometry was performed on the cells collected in the BAL samples. *N. brasiliensis* infection stimulates a polarized Th2 immune response in the host which includes recruitment of eosinophils to the lungs, and therefore, eosinophils were strongly considered when the flow cytometry experiments were performed.[9,28,29] BAL eosinophils and alveolar macrophages were gated based on surface expression for SiglecF and CD11c.[30] Alveolar macrophages were gated
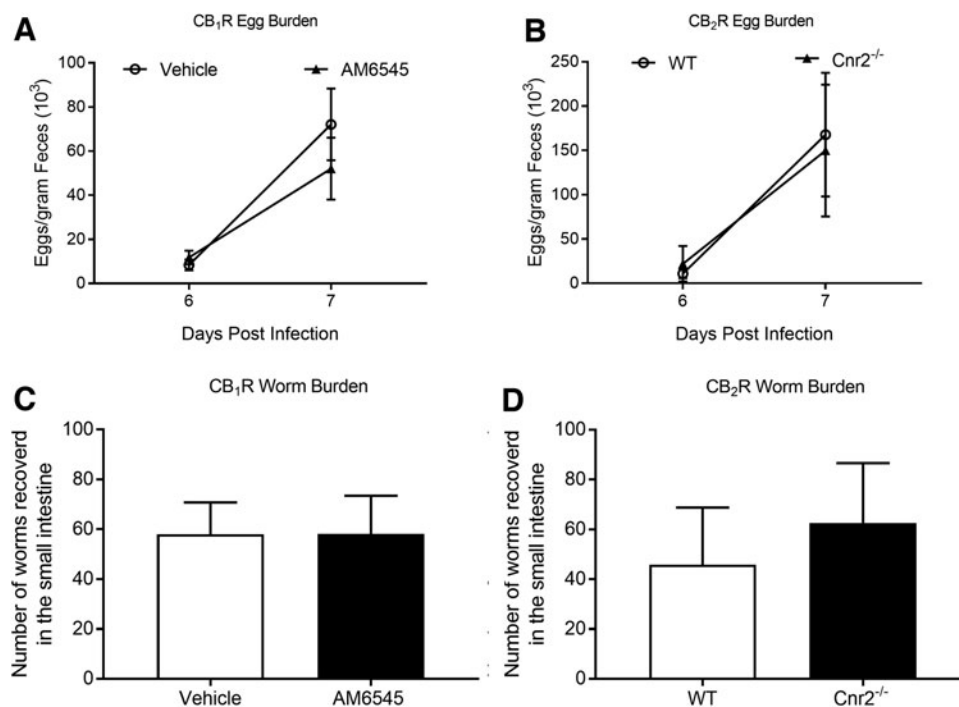

FIG. 5. Egg burden of infected mice at 6 and 7 DPI indicated no change in parasite fecundity irrespective of treatment or genotype [(**A, B**): $n = 18$, veh; $n = 21$, AM6545; $n = 13$, WT; $n = 14$, Cnr2$^{-/-}$]. No change in worms recovered from the small intestine was observed across treatment or genotype [(**C, D**): $n = 18$, veh; $n = 21$, AM6545; $n = 13$, WT; $n = 14$, Cnr2$^{-/-}$]. Repeated measures two-way ANOVA with Sidak's multiple comparison *post hoc* test (**A, B**); unpaired two-tailed student's *t*-test (**C, D**). Results are expressed as mean $\pm$ SEM.

as SiglecF$^+$CD11c$^+$, while eosinophils were SiglecF$^+$ CD11c$^-$ as displayed in the representative flow plots from each condition (Fig. 4A–D). Alveolar macrophages were the main cell population in the naive BAL, and frequency was reduced following *N. brasiliensis* infection due to an increase in infiltrating eosinophils (Fig. 4G, J); however, no changes in number of macrophages were observed across any condition (data not shown). Compared to vehicle treatment in *N. brasiliensis* infected mice, treatment with AM6545 throughout infection significantly increased the frequency (Fig. 4E, from $10.7 \pm 1.6\%$ to $16.1 \pm 1.9\%$; $n = 21$, $p < 0.01$) and number (Fig. 4F, from $1.8e3 \pm 3.3e2$ cells to $3.6e3 \pm 6.4e2$ cells; $n = 20$ and 21, $p < 0.01$) of eosinophils recovered in BAL samples. Compared to infected WT mice, no changes were found in infected Cnr2$^{-/-}$ for percent (Fig. 4H, from $12.59 \pm 3.424\%$ to $11.62 \pm 3.734\%$; $n = 10$; $p = 0.964$) or number (Fig. 4I, from $4.6e3 \pm 1.7e3$ cells to $4.4e3 \pm 1.6e3$ cells; $n = 9/10$, respectively; $p = 0.995$) of eosinophils recovered in BAL. These data further suggest that deficiencies in CB$_1$R signaling in the lung promote host-destructive Th2 inflammatory processes in *N. brasiliensis* infection, while constitutive activity at CB$_1$Rs in the lung may provide protection during infection. A direct test of this hypothesis, however, remains for future studies.

Parasite burden is unaffected by inhibition of CB$_1$Rs or in Cnr2$^{-/-}$ mice

Adulthood is established by *N. brasiliensis* in the small intestine where fertilized eggs are released into the fecal matter as early as 6 DPI.[11] To identify the fecundity of *N. brasiliensis* when host CB$_1$R or CB$_2$R is inhibited, fecal egg burden was quantified at 6 and 7 DPI. Compared to vehicle treatment in mice infected with *N. brasiliensis*, treatment with AM6545 throughout *N. brasiliensis* infection had no effect on egg burden by 6 DPI (Fig. 5A, from 9.89 ± 2.87 eggs/g [10^3] to 11.78 ± 3.0 eggs/g [10^3], $p = 0.831$) and 7 DPI (from 72.12 ± 16.22 eggs/g [10^3] to 54.72 ± 14.83 eggs/g [10^3], $p = 0.369$). Similarly, compared to infected WT mice, no changes in egg burden were found in infected Cnr2$^{-/-}$ mice by 6 DPI (Fig. 5B, from 10.876 ± 5.043 eggs/g [10^3] to 22.035 ± 20.122 eggs/g [10^3], $p = 0.896$) and 7 DPI (from 167.849 ± 69.775 eggs/g [10^3] to 149.928 ± 20.122 eggs/g [10^3], $p = 0.897$). Moreover, compared to vehicle treatment in mice infected with *N. brasiliensis*, no changes were observed in parasite burden in mice treated with AM6545 (Fig. 5C, from 58 ± 15 to 58 ± 13 worms, $p = 0.996$). In addition, no changes in parasite burden were observed between

infected WT and Cnr2$^{-/-}$ mice (Fig. 5D, from 46 ± 23 to 63 ± 24 worms, $p = 0.626$). In contrast to this current study where peripheral CB$_1$Rs were also blocked early during the lung phase of infection, our previously reported study indicated that blockade of peripheral CB$_1$R signaling in the intestinal phase of infection (4–7 DPI) exacerbated egg burden at 8 DPI only with no changes in worm burden.[10] Similarly, no changes in worm burden were observed in the current study in mice receiving daily administration of AM6545 throughout *N. brasiliensis* infection; however, the increase in parasite fecundity was ablated. This result suggests a possible role for CB$_1$R signaling in the lung phase of infection (1–4 DPI) in these processes, which may lead to changes in parasite fertility. Furthermore, we recently reported that *N. brasiliensis* is capable of producing eCBs, which peak in concentration during the lung phase of infection.[10] These parasite-derived eCBs may be acting on host CB$_1$Rs to mediate the immune response in the microenvironment; future studies designed to directly test this hypothesis and the mechanism(s) involved are warranted.

Conclusions

These studies suggest an immunomodulatory role for CB$_1$Rs in host-destructive inflammatory responses to parasitic infections (Table 1). Prolonged eosinophilia

Table 1. Inhibition of Peripheral Cannabinoid Receptor Subtype-1s with AM6545 Increases Lung Hemorrhaging, Excessive Populations of SiglecF$^+$CD11c$^-$ Eosinophils in the Lungs, and Lung Tissue Damage During *Nippostrongylus brasiliensis* Infection

	Peripheral CB$_1$R blockade	Global Cnr2$^{-/-}$
Hemorrhaging	↑	—
Lung eosinophilia	↑	—
Lung tissue damage	↑	—
Parasite burden	—	—

No changes were observed in any of the measured parameters in CB$_2$R-null mice infected with *Nippostrongylus brasiliensis* compared to WT infected mice. Despite the evidence for an enhanced immune response to infection when peripheral CB$_1$R signaling is inhibited, there is no change in parasite burden or parasite fecundity suggesting an immunomodulatory role for CB$_1$R signaling in response to *N. brasiliensis* infection. Collectively, these data suggest a host-protective role for CB$_1$Rs in parasitic helminth infection.

CB$_1$R, cannabinoid receptor subtype-1; CB$_2$R, cannabinoid receptor subtype-2; WT, wild-type.

may contribute to exacerbated host tissue damage in mice treated with the CB₁R inhibitor, AM6545; however, the specific mechanism(s) in this response remains to be identified. Despite the well-defined roles for the eCB system in nutrient seeking and sensing, no changes in feeding behavior were observed when CB₁R or CB₂R signaling was disrupted throughout infection. Moreover, the increase in infection-induced inflammatory processes in mice treated with AM6545 was not associated with altered parasite clearance, which suggests that blockade of CB₁R signaling during the lung phase of infection may not impact parasite burden. Nonetheless, it is possible that metabolism of eCBs may contribute to eicosanoid formation, which can act as a chemoattractant to immune cells and contribute to prolonged eosinophilia in the lungs of AM6545-treated mice. Future research should consider eicosanoid formation and signaling in conjunction with CB₁R signaling in immune cells to control immune cell trafficking. Collectively, these studies provide further insight into the role for CB₁R signaling in the Th2 response and parasitic infections.

Limitations

We investigated roles for the eCB system in parasite-induced lung injury and repair. Given that inhibition of peripheral CB₁Rs exacerbated lung injury during infection, future studies should consider if activation of CB₁Rs improves outcomes and provides further host protection. In addition, the functional target for AM6545 in mediating this host protection remains unclear, and future studies are needed to delineate the function of CB₁R signaling on immune or resident cells in the lung. Finally, *N. brasiliensis* is a natural parasite of rats and not mice; therefore, studies using mouse-adapted parasites may provide more physiologic insight into how the eCB system influences parasite clearance, which can be better translated to human helminth infections.

Supplementary Material
Supplementary Figure S1

References

1. Weatherhead JE, Hotez PJ, Mejia R. The global state of helminth control and elimination in children. J Pediatr Clin North Am. 2017;64:867–877.
2. Bouchery T, Filbey K, Shepherd A, et al. A novel blood-feeding detoxification pathway in *Nippostrongylus brasiliensis* L3 reveals a potential checkpoint for arresting hookworm development. PLoS Pathog. 2018;14:e1006931.
3. Hotez PJ. Neglected infections of poverty in the United States of America. PLoS Negl Trop Dis. 2008;2:e256.
4. Batugedara HM, Li J, Chen G, et al. Hematopoietic cell-derived RELMα regulates hookworm immunity through effects on macrophages. J Leukoc Biol. 2018;104:855–869.
5. Pine GM, Batugedara HM, Nair MG. Here, there and everywhere: resistin-like molecules in infection, inflammation, and metabolic disorders. Cytokine. 2018;110:442–451.
6. Holgate ST. Innate and adaptive immune responses in asthma. Nat Med. 2012;18:673–683.
7. Hirahara K, Shinoda K, Morimoto Y, et al. Immune cell-epithelial/mesenchymal interaction contributing to allergic airway inflammation associated pathology. Front Immunol. 2019;10:570.
8. Jang JC, Chen G, Wang SH, et al. Macrophage-derived human resistin is induced in multiple helminth infections and promotes inflammatory monocytes and increased parasite burden. PLoS Pathog. 2015;11:e1004579.
9. Knott ML, Matthaei KI, Foster PS, et al. The roles of eotaxin and the STAT6 signalling pathway in eosinophil recruitment and host resistance to the nematodes *Nippostrongylus brasiliensis* and *Heligmosomoides bakeri*. Mol Immunol. 2009;46:2714–2722.
10. Batugedara HM, Argueta D, Jang JC, et al. Host and helminth-derived endocannabinoids are generated during infection with effects on host immunity. Infect Immun. 2018;86:00441-18.
11. Hawdon JM, Hotez PJ. Hookworm: developmental biology of the infectious process. Curr Opin Genet Dev. 1996;6:618–623.
12. Roulette CJ, Kazanji M, Breurec S, et al. High prevalence of cannabis use among Aka foragers of the Congo Basin and its possible relationship to helminthiasis. Am J Hum Biol. 2016;28:5–15.
13. DiPatrizio NV. Endocannabinoids in the gut. Cannabis Cannabinoid Res. 2016;1:67–77.
14. DiPatrizio NV, Piomelli D. The thrifty lipids: endocannabinoids and the neural control of energy conservation. Trends Neurosci. 2012;35:403–411.
15. Avalos B, Argueta DA, Perez PA, et al. Cannabinoid CB1 receptors in the intestinal epithelium are required for acute western-diet preferences in mice. Nutrients. 2020;12:2874.
16. Galiègue S, Mary S, Marchand J, et al. Expression of central and peripheral cannabinoid receptors in human immune tissues and leukocyte subpopulations. Eur J Biochem. 1995;232:54–61.
17. Larose MC, Turcotte C, Chouinard F, et al. Mechanisms of human eosinophil migration induced by the combination of IL-5 and the endocannabinoid 2-arachidonoyl-glycerol. J Allergy Clin Immunol. 2014;133:1480–1482, 1482.e1–e3.
18. Powell WS, Rokach J. The eosinophil chemoattractant 5-oxo-ETE and the OXE receptor. Prog Lipid Res. 2013;52:651–665.
19. Kaplan BL, Lawver JE, Karmaus PW, et al. The effects of targeted deletion of cannabinoid receptors CB1 and CB2 on intranasal sensitization and challenge with adjuvant-free ovalbumin. Toxicol Pathol. 2010;38:382–392.
20. Pandey R, Mousawy K, Nagarkatti M, et al. Endocannabinoids and immune regulation. Pharmacol Res. 2009;60:85–92.
21. Nagarkatti P, Pandey R, Rieder SA, et al. Cannabinoids as novel anti-inflammatory drugs. Future Med Chem. 2009;1:1333–1349.
22. Meng F, Alayash AI. Determination of extinction coefficients of human hemoglobin in various redox states. Anal Biochem. 2017;521:11–19.

23. Marsland BJ, Kurrer M, Reissmann R, et al. *Nippostrongylus brasiliensis* infection leads to the development of emphysema associated with the induction of alternatively activated macrophages. Eur J Immunol. 2008;38:479–488.

24. Chen CM, Hwang J, Chou HC, et al. Anti-Tn monoclonal antibody attenuates hyperoxia-induced lung injury by inhibiting oxidative stress and inflammation in neonatal mice. Front Pharmacol. 2020;11:568502.

25. Sutherland TE, Rückerl D, Logan N, et al. Ym1 induces RELMα and rescues IL-4Rα deficiency in lung repair during nematode infection. PLoS Pathog. 2018;14:e1007423.

26. Reece JJ, Siracusa MC, Scott AL. Innate immune responses to lung-stage helminth infection induce alternatively activated alveolar macrophages. Infect Immun. 2006;74:4970–4981.

27. Cinar R, Gochuico BR, Iyer MR, et al. Cannabinoid CB1 receptor overactivity contributes to the pathogenesis of idiopathic pulmonary fibrosis. JCI Insight 2017;2:e92281.

28. Chen F, Liu Z, Wu W, et al. An essential role for TH2-type responses in limiting acute tissue damage during experimental helminth infection. Nat Med. 2012;18:260–266.

29. Anthony RM, Rutitzky LI, Urban JF, et al. Protective immune mechanisms in helminth infection. Nat Rev Immunol. 2007;7:975–987.

30. Stevens WW, Kim TS, Pujanauski LM, et al. Detection and quantitation of eosinophils in the murine respiratory tract by flow cytometry. J Immunol Methods. 2007;327:63–74.

Abbreviations Used

2-AG = 2-arachidonoyl-sn-glycerol
ANOVA = analysis of variance
BAL = bronchoalveolar lavage
CB_1R = cannabinoid receptor subtype-1
CB_2R = cannabinoid receptor subtype-2
DPI = days postinfection
eCB = endocannabinoid
MLI = mean linear intercept
PBS = phosphate buffered saline
PFA = paraformaldehyde
SEM = standard error of the mean
Th2 = T-helper type 2
WT = wild-type